Cosolvent-Induced Aggregation Inhibits Myosin ATPase Activity by Stabilizing the Predominant Transition Intermediate†

Y. Michael Peyser,‡ Shirley Shaya,‡ Katalin Ajtai,§ Thomas P. Burghardt,§ and Andras Muhlrad*,‡

Department of Oral Biology, Hebrew University−Hadassah School of Dental Medicine, Jerusalem, Israel 91120, and Department of Biochemistry and Molecular Biology, Mayo Foundation, Rochester, Minnesota 55905

Received June 12, 2003; Revised Manuscript Received August 31, 2003

ABSTRACT: High concentration of the cosolvent poly(ethylene glycol) (PEG) induces reversible aggregation of skeletal myosin subfragment 1 (S1) and inhibition of its Mg-ATPase activity [Highsmith et al. (1998) *Biophys. J. 74*, 1465−1472]. In the present work the effect of aggregation on the various steps of the ATPase cycle was studied. The isomerization and hydrolysis steps of the cycle were not affected by S1 aggregation since the formation of the "trapped" S1·MgADP·phosphate analogue complexes, which mimic the prehydrolysis M*ATP and posthydrolysis M**ADP·P_i transition states, proceeded without any hindrance. Similar conclusions could be reached from the chemical modification of Lys-83 and Cys-707 in the presence of MgATP and MgATPγS, which indicated that the most populated intermediate of the cycle in solubilized and aggregated S1 is M**ADP·P_i. The dissociation of the trapped S1·MgADP·phosphate analogue complexes resembling the M**ADP·P_i state was strongly inhibited by PEG-6000, showing that the transition from this intermediate is prevented by the aggregation. This step is presumably inhibited because the coupled swinging of the lever arm from the closed to the open position is constrained by the close packing of aggregated S1.

Contraction of skeletal muscle is based on the interaction of the myosin motor with actin, which is powered by the coupled hydrolysis of ATP. The globular head of myosin, called subfragment 1 or S1, where both the nucleotide and actin binding sites of the molecule are located, is responsible for the generation of force during contraction. Crystallographic studies revealed that S1[1] is made up of an N-terminal catalytic domain containing the actin and ATP binding sites and a C-terminal lever arm domain consisting of an α-helix (*1*−*4*). During ATP hydrolysis S1 accomplishes an ∼70 deg rotation of the lever arm α-helix while keeping much of the catalytic and lever arm domains roughly intact. This large conformation change occurs due to substantial secondary structure transformation localized in switch 2, the switch 2 helix and loop, and at the glycine swivel, Gly-699 [reviewed by Geeves and Holmes (*5*)]. The catalytic domain is attached to actin at a fixed position and does not perform global movement during the power stroke of the cross-bridge cycle. The lever arm rotation is also coupled to the Mg-mediated ATP hydrolysis in the absence of actin, which can be described according to Bagshaw and Trentham (*6*) by the simplified Scheme 1, where M is myosin subfragment 1 and M, M*·ATP, M**·ADP·P_i, and M*ADP represent conformational states of S1−nucleotide complexes with distinct structural and spectral properties.

Scheme 1

$$M + ATP \overset{1}{\leftrightarrow} M\cdot ATP \overset{2}{\leftrightarrow} M^*\cdot ATP \overset{3}{\leftrightarrow} M^{**}\cdot ADP\cdot P_i \overset{4}{\leftrightarrow} M^*\cdot ADP \overset{5}{\leftrightarrow} M\cdot ADP \overset{6}{\leftrightarrow} M + ADP$$

The crystallization of S1 with and without nucleotides provided the most detailed evidence that S1 exists in well-defined distinct conformational states in the various stages of the ATPase cycle (*5*). While the structures obtained from different isoforms of myosin II (*Dictyostelium*, smooth muscle, scallop) varied somewhat, most of them fell into three main classes defined by the relative positions of the catalytic and lever arm domains. The first class is the "near rigor state", which represents the apo (M) form of S1. The second class is the "open" state, which is favored by nonhydrolyzable ATP analogues, such as ATPγS or AMP-PNP, and also by ADP·BeF_x. In general, it corresponds to the prehydrolysis M*·ATP state and is characterized by an extended lever arm. The third class, i.e., the "closed" state, is favored by the analogues of the posthydrolysis M**·ADP·P_i transition state (ADP·V_i or ADP·AlF_4). In this state the lever arm and catalytic domain form a more compact conformation as a result of a 70 deg swing of the lever arm. On the basis of the determined atomic structures one can view Scheme 1 as transitions between closed and open states. The open to closed transition occurs in step 3 and the closed to open transition in step 4.

In addition to crystallographic evidence solution studies also indicated shape changes in S1 during various stages of

† This research was supported by the Israel Science Foundation (Grant 230/99 to A.M.), by the National Institutes of Health (Grant R01 AR39288 to T.P.B.), and by the Mayo Foundation.

* Corresponding author: e-mail, Muhlrad@cc.huji.ac.il.

‡ Hebrew University−Hadassah School of Dental Medicine.

§ Mayo Foundation.

[1] Abbreviations: PEG, poly(ethylene glycol); S1, myosin subfragment 1; P_i, inorganic phosphate; V_i, vanadate; BeF_x, beryllium fluoride complex; AlF_4, aluminum fluoride complex; TNBS, 2,4,6-trinitrobenzenesulfonate; IAEDANS, *N*-iodoacetyl-*N*′-(5-sulfo-1-naphthyl)ethylenediamine; DTT, dithiothreitol; ATPγS, adenosine 5′-*O*-thiotriphosphate.

10.1021/bi0350093 CCC: $25.00
Published on Web 10/04/2003

ATP hydrolysis. These have been shown by electric birefringence (*7*), by X-ray and neutron scattering (*8*), and by probes, which can indicate the movement of the lever arm (*9*−*11*).

Highsmith et al. (*12*) have shown that addition of a high molecular weight cosolvent, poly(ethylene glycol) (PEG), causes reversible aggregation of S1. This aggregation, caused by the addition of 20% PEG compared to the 3−12% used to promote S1 crystallization (*2*, *3*), is accompanied by the reversible loss of the Mg-mediated ATPase activity measured at low ionic strength. According to the authors ATPase activity inhibition is caused by the aggregation that prevents segmental motions coupled to nonidentified steps of ATP hydrolysis. Grazi et al. (*13*) did not accept the above explanation and proposed that the inhibition of the Mg-ATPase activity of S1 is due to chelation of Mg by the high molecular weight PEG. In response to Grazi and co-workers' criticism, Highsmith et al. (*14*) showed that the inhibition of Mg-ATPase is independent of Mg concentration in the 1−10 mM range. However, the step in the ATPase activity, which was inhibited at high PEG concentration, was not identified.

In this study we attempted to clarify the mechanism of the PEG inhibition of the S1 ATPase activity by finding out whether the closed to open or the open to closed transition or both are affected in the ATPase cycle (Scheme 1) by PEG. We found in accordance with Highsmith et al. (*12, 14*) that the inhibition of Mg-ATPase activity is independent of the Mg concentration, and high ionic strength abolishes the S1 aggregation and the inhibition of the Mg-ATPase activity. By using phosphate analogues and chemical modifications, we identified the step in the ATPase cycle inhibited by aggregation. Our results indicate that PEG does not influence the binding or hydrolysis of ATP but inhibits the release of phosphate from the M**·ADP·P_i transition state complex. Presumably, this occurs because aggregation prevents the swinging of the lever arm from bent to extended position (closed to open transition), which is coupled to the phosphate release.

MATERIALS AND METHODS

Chemicals. ATP, ADP, TNBS, DTT, PEG-3000, PEG-6000, phenylmethanesulfonyl fluoride, chymotrypsin, HEPES, and Tris-HCl were purchased from Sigma Chemical Co. IAEDANS was purchased from Molecular Probes Inc., Eugene, OR. ATPγS was from Boehringer Mannheim (Indianapolis, IN). All other chemicals were of reagent grade.

Proteins. Myosin was prepared from the back and leg muscles of rabbit by the methods of Tonomura et al. (*15*). S1 was obtained by digestion of myosin filaments with chymotrypsin following the procedure of Weeds and Taylor (*16*). S1 concentration was estimated from its absorption by using an $A^{1\%}$ at 280 nm of 7.5 cm^{-1}. The molecular mass of S1 was assumed to be 115 kDa.

ATPase Activity Assays. Mg-, Ca-, and K(EDTA)-activated S1 ATPase activities (micromoles of phosphate per micromole of S1 per second) were calculated from the inorganic phosphate produced, assayed by a Malachite green method (*17*). The reactions were performed at 25 °C. Incubation times were chosen so that no more than 15% of the ATP was hydrolyzed. Mg-mediated ATPase activity, which was measured at low ionic strength, contained 1−2 μM S1 in the presence and absence of PEG in 0−10 mM $MgCl_2$, 25 mM HEPES buffer, pH 7.0, and 1 mM ATP. At different $MgCl_2$ concentrations the ionic strength of the assay buffer was adjusted by adding KCl. K(EDTA)- and Ca-activated ATPase activities were assayed at high ionic strength (0.5−0.6 M KCl). Under these ionic conditions the PEG-aggregated S1 was solubilized. The aggregation by PEG and the following solubilization essentially did not affect the ATPase activity of S1. K(EDTA)-activated ATPase activity was measured in solutions of 0.2 μM S1, 6 mM EDTA, 600 mM KCl, 50 mM Tris-HCl buffer, pH 8.0, and 2 mM ATP. Ca-activated ATPase activity was assayed in solutions of 0.2 μM S1, 5 mM $CaCl_2$, 500 mM KCl, 50 mM Tris-HCl buffer, pH 8.0, and 2 mM ATP.

Light Scattering Measurements. Aggregation of 0.5 μM S1 by PEG-3000 and PEG-6000 was assessed by the increase in light scattering. The measurements were performed in a PTI spectrofluorometer (Photon Technology International). Both emission and excitation wavelengths were set at 400 nm.

Formation of Stable S1·ADP·Phosphate Analogue Complexes (Trap Formation). This was carried out essentially according to Peyser et al. (*18*). S1 (17−30 μM) in the presence or absence of 20% PEG-6000 was incubated in 1 mM $MgCl_2$ and 20 mM HEPES buffer, pH 7.0, at 25 °C with 0.2 mM ADP for 5 min. In the case of BeF_x- or AlF_4-containing complexes 5 mM NaF was also present. After that 0.2 mM V_i, $BeCl_2$, or $AlCl_3$ was added, and the incubation was continued at 25 °C for 20 min. To study the course of formation of the "trapped" complexes, aliquots were taken at selected time intervals after addition of phosphate analogues in order to assay the K^+(EDTA)-activated ATPase activity.

Dissociation of the Stable S1·MgADP·Phosphate Analogue Complexes. This was carried out essentially according to Peyser et al. (*18*) by EDTA chase. The metal ions, which have been dissociated from the S1·MgADP·phosphate analogue complex, are chelated with EDTA that reacts only with free Mg^{2+} but not with Mg^{2+} trapped in the complex. The EDTA-chelated Mg^{2+} cannot reenter the complex, which dissociates in the absence of divalent cation. Following trap formation the S1·MgADP·phosphate analogue complex was filtered through a spin column to remove reagent excess. After that the trapped complex was incubated at 25 °C in the presence or absence of 20% PEG-6000 with 4 mM EDTA, and its dissociation was followed by measuring the recovery of the K(EDTA)-activated ATPase activity as described above.

Effect of Trinitrophenylation of Lys-83 on the ATPase Activity of S1. The time course of Lys-83 trinitrophenylation was followed by monitoring the decrease in the K(EDTA)-activated ATPase activity of S1. TNBS (final concentration 100 μM) was added to 10 μM S1 in the presence or absence of 20% PEG-6000 and nucleotides (4 mM ATP, 0.2 mM ATPγS) in 1 mM $MgCl_2$ and 30 mM Tris-HCl, pH 8.0. Aliquots were taken at selected time intervals after addition of TNBS, and the reaction was quenched by 0.5 mM DTT. Finally, the K(EDTA)-activated ATPase activity of the aliquots was measured.

Effect of Alkylation of Cys-707 (SH_1) on the Ca-Activated ATPase Activity of S1. The time course of the reaction of

Table 1: Mg^{2+} Dependence of S1 Mg-ATPase Activity Inhibition by PEG[a]

	Mg-ATPase activity (s^{-1})	
Mg^{2+} (mM)	no PEG	20% PEG-6000
1.0	0.033	0.0041
3.0	0.033	0.0042
6.0	0.034	0.0046
10.0	0.034	0.0047

[a] For details of the ATPase activity assay, see Materials and Methods.

Cys-707 (SH_1) with IAEDANS was followed by assaying the increase in the Ca-activated ATPase activity of S1. IAEDANS (in 20 μM final concentration) was added to 10 μM S1 in the presence or absence of 20% PEG-6000 and nucleotides (4 mM ATP, 0.2 mM ATPγS) in 0.5 mM $MgCl_2$ and 30 mM Tris-HCl, pH 8.0. At selected time intervals after addition of IAEDANS aliquots were taken into 0.5 mM DTT, 500 mM KCl, and 10 mM Tris-HCl in order to quench the reaction and abolish the effect of 20% PEG-6000. Finally, the Ca-activated ATPase activity was assayed.

S1 Volume and Surface Area Calculation. S1 volume and surface area were computed using quantitative structure−activity relationships (QSAR) software implemented in HyperChem (Hypercube, Inc., Gainesville, FL). The volume and surface area calculations use a method described by Bodor et al. (*19*) and the solvent-accessible surface option with a solvent probe radius of 3 Å. The protein structures are the skeletal S1 sequence, homology modeled into the M, M*, and M** conformations using the skeletal (*20*), scallop (*3*), and smooth muscle myosin (*2*) crystal structures, respectively. Homology modeling was done with Modeller (*21*) on a sequence containing the skeletal heavy chain and essential light chain. The homology models contain flexible loops and other peptides missing from the crystal structures that are inserted and energy minimized according to the Modeller protocol. The skeletal M, M*, and M** structures have identical sequence and molecular weights.

RESULTS

Mg Dependence of the PEG Inhibition of S1 ATPase Activity. There is a controversy on the cause of the PEG inhibition of Mg-modulated S1 ATPase activity. According to Grazi et al. (*13*) it is caused by the PEG chelation of free Mg ions, while Highsmith et al. (*14*) showed that the inhibition is due to PEG-induced S1 aggregation. Because of this controversy we tested the Mg dependence of the PEG inhibition. The Mg-ATPase activity of S1 was measured in the 1−10 mM Mg range in the presence and absence of 20% PEG-6000. The ionic strength was kept constant at each point by addition of KCl because increasing ionic strength has been shown to reduce the PEG inhibition of Mg-ATPase activity (*12*). According to our results, in agreement with Highsmith et al. (*14*), 20% PEG-6000 strongly inhibits the Mg-ATPase activity of S1 independently of Mg concentration in the 1−10 mM range (Table 1). This excludes the possibility that the PEG inhibition of S1 ATPase activity is due to the chelation of free Mg.

Effect of Ionic Strength on the PEG-Induced Aggregation and ATPase Activity Inhibition of S1. The effect of ionic strength on S1 aggregation caused by 25% PEG-3000 or PEG-6000 was studied by monitoring the light scattering of

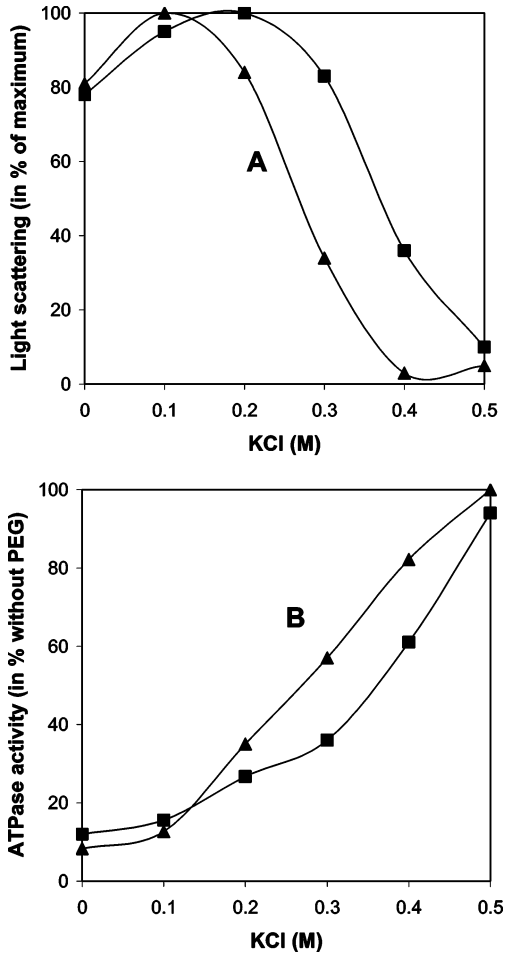

FIGURE 1: Effect of ionic strength on the PEG-induced light scattering increase and Mg-ATPase activity inhibition of S1. (A) Light scattering of 0.5 μM S1 in 25% PEG-3000 (▲) or PEG-6000 (■), 25 mM MOPS buffer, and 1 mM $MgCl_2$ was measured in the presence of increasing KCl concentration. (B) Mg-ATPase activity of 1 μM S1. S1 in 25% PEG-3000 (▲) or PEG-6000 (■), 25 mM MOPS buffer, and 1 mM $MgCl_2$ was assayed in the presence of increasing KCl concentration as described in Materials and Methods.

S1 in the presence of increasing concentrations of KCl (Figure 1A). KCl (0.5 M) completely abolished the light scattering increase induced by both PEG-3000 and PEG-6000 essentially as observed by Highsmith et al. (*12*). However, significantly less KCl was needed for the decrease of light scattering in the case of PEG-3000 than with PEG-6000. The PEG inhibition of the Mg-ATPase activity of S1 also decreased by the increasing KCl concentration (Figure 1B). Similarly to the light scattering change, KCl was more efficient in abolishing the PEG-3000- than the PEG-6000-caused inhibition of S1 ATPase activity. These data show that it is not just the presence of PEG, but the PEG-induced aggregation, that causes inhibition of the ATPase activity. The finding that KCl is more efficient in reversing aggregation by PEG-3000 than by PEG-6000 indicates that the PEG exclusion volume plays a role in the mechanism of S1 aggregation (*22*). Volume exclusion due to PEG was shown to influence the solubility of several different proteins (*23*). Presumably, KCl perturbs the attractive electrostatic interactions between the S1 molecules. This indicates that both volume exclusion and ionic interaction have a role in the aggregation of S1 by the PEG cosolvent.

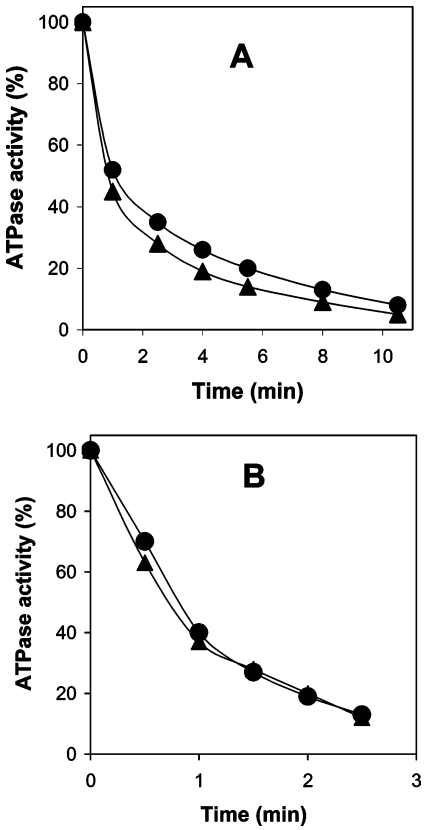

FIGURE 2: Time course of formation of trapped S1·MgADP·phosphate analogue complexes in the presence of 20% PEG-6000. The time course of complex formation was followed by assaying the K(EDTA)-activated ATPase activity of S1 as described in Materials and Methods. Symbols: (●) 20% PEG-6000; (▲) no PEG present. ATPase activities expressed as a percentage of activity of S1 in the absence of phosphate analogue. (A) S1·MgADP·V_i and (B) S1·MgADP·BeF_x formation.

Effect of PEG on the Formation of Trapped S1·MgADP·Phosphate Analogue Complexes. Highsmith et al. (*12*) showed that ATP binds to S1 also in the presence of PEG, but the S1−nucleotide complex formed in the ATPase cycle (Scheme 1) under these conditions was not defined unambiguously. A convenient way to study the nature of the S1−nucleotide complex is to follow the trapping of phosphate analogues in the presence of Mg and ADP (*18*). We monitored the formation of M*ATP (S1·MgADP·BeF_x) and M**ADP·P_i (S1·MgADP·V_i and S1·MgADP·AlF_4) mimicking complexes (*24*, *25*) in the presence and absence of 20% PEG by assaying the decrease in K(EDTA)-activated ATPase activity (Figure 2). This ATPase activity was assayed because it was measured at high ionic strength, and therefore, it was not inhibited by the 20% PEG concentration (Figure 1 and ref *12*). The time course of trapping, revealed by the decrease in ATPase activity, was essentially identical in both the presence and absence of 20% PEG-6000 with each phosphate analogue (only V_i and BeF_x are shown in Figure 2). The finding that PEG does not inhibit trapping indicates that the isomerization of M·ATP to M*·ATP and its hydrolysis to M**ADP·P_i proceed also in PEG-induced aggregation conditions. It follows that either the M*ATP or the M**ADP·P_i state is predominant in the ATPase cycle (Scheme 1) in the presence of 20% PEG-6000. However, further experiments were needed to determine which state is predominant in the presence of PEG.

Table 2: Rates of Dissociation of S1·MgADP·Phosphate Analogue Complexes in the Presence of 20% PEG-6000[a]

S1·MgADP·phosphate analogue complex	ATPase activity recovery (% h^{-1})	
	no PEG	20% PEG-6000
S1·MgADP·V_i	3.54	1.18
S1·MgADP·AlF_4	5.98	1.37
S1·MgADP·BeF_x	1.66	1.25

[a] Rates of dissociation were calculated from the initial phase of recovery of the K(EDTA)-activated ATPase activity of S1 following EDTA chase. Details of the method are given in Materials and Methods.

Effect of PEG on the Dissociation of Trapped S1·MgADP·Phosphate Analogue Complexes. Our aim was to define whether transition from the open prehydrolysis M*ATP or from the closed posthydrolysis M**ADP·P_i state is inhibited in the ATPase cycle in the presence of PEG. To accomplish this, we mimicked the M*ATP state by S1·MgADP·BeF_x and the M**ADP·P_i state by S1·MgADP·V_i or S1·MgADP·AlF_4 trapped complexes as described above and measured their rate of dissociation by EDTA chase (*18*). The recovery of the K(EDTA)-activated ATPase activity of S1 indicated the dissociation of the trapped complex in these measurements. The rate of dissociation of all of the trapped complexes was inhibited by the presence of PEG (Table 2). However, the dissociation of the S1·MgADP·V_i and S1·MgADP·AlF_4 trapped complexes was strongly inhibited, while the slow dissociation of S1·MgADP.BeF_x was much less affected by PEG. Since both S1·MgADP·V_i and S1·MgADP·AlF_4 mimic the M**ADP·P_i closed state, our results indicate that step 4 in Scheme 1 is inhibited by the PEG -induced aggregation and that in the presence of 20% PEG-6000 the M**ADP·P_i transition state is the most populated in the ATPase cycle.

Trinitrophenylation of Lys-83 of S1 in PEG. Lys-83 is the most reactive lysine residue of the myosin head (*26*) located in the 27 kDa N-terminal segment of the molecule (*27*, *28*) at an interface of the converter and lever arm domains (*29*). 2,4,6-Trinitrobenzenesulfonate (TNBS) preferentially trinitrophenylates Lys-83. The rate of modification of Lys-83 is 3 orders of magnitude faster than for the rest of the lysine residues of S1 (*30*). The reaction of this fast-reacting lysine with TNBS causes dramatic increase in Mg-activated and decrease in K(EDTA)-activated ATPase activity of S1 (*26*, *31*) and the loss of myosin motor function (*32*), while the reaction of other, slowly reacting lysines essentially does not affect the ATPase activity or function. The modification of Lys-83 is strongly inhibited by nucleotides (*33*, *34*), which was also observed in the present work by monitoring the effect of Lys-83 modification on the K(EDTA)-activated ATPase activity of S1 (Figure 3A,B). On the basis of the extent of S1 protection against modification of Lys-83 the nucleotides could be classified into two groups. Those nucleotides, like MgATPγS, which favor the structure of S1 resembling the open M*ATP state (*35*), protect less, while those like MgATP, for which the closed M**·ADP·P_i transition state is the most populated, protect S1 more (*29*). We studied the trinitrophenylation of Lys-83 and the effect of MgATPγS and MgATP on the modification in the presence of 20% PEG-6000 by monitoring the decrease in K(EDTA)-activated ATPase activity (assayed at high ionic strength when there is no PEG inhibition) during the course of the reaction (Figure 3). We found that the S1 aggregation

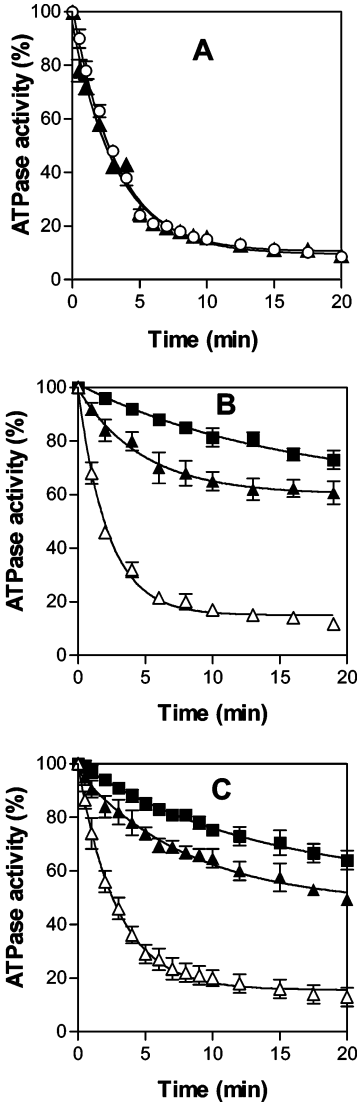

FIGURE 3: Effect of Lys-83 trinitrophenylation on the K(EDTA)-activated ATPase activity of S1 in the presence of 20% PEG-6000. Following addition of TNBS the K(EDTA)-activated ATPase activity of S1 was measured as described in Materials and Methods. The ATPase activity is expressed as a percentage of the unmodified S1 activity. (A) Trinitrophenylation of the apo form of S1 in the absence of nucleotides. Symbols: (▲) 20% PEG-6000; (○) no PEG present. Trinitrophenylation in the presence (B) and in the absence (C) of PEG. Symbols: (■) 4 mM ATP; (▲) 0.2 mM ATPγS; (△) no nucleotide present.

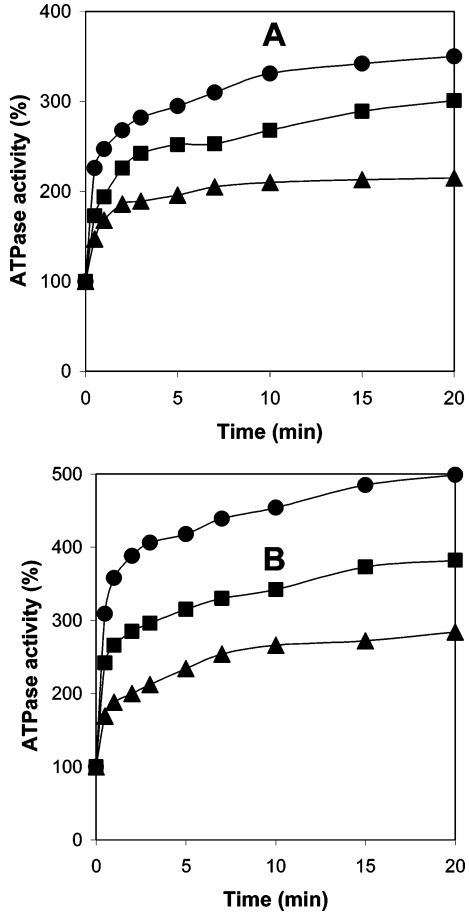

FIGURE 4: Effect of alkylation of Cys-707 (SH_1) on the Ca-activated ATPase of S1 in the presence of 20% PEG-6000. Following the addition of IAEDANS the Ca-activated ATPase of S1 was measured as described in Materials and Methods. The ATPase activity is expressed as a percentage of the unmodified S1 activity. Alkylation in the presence (A) and in the absence (B) of PEG. Symbols: (■) 4 mM ATP; (●) 0.2 mM ATPγS; (▲) no nucleotide present.

caused by PEG essentially did not influence the rate and extent of Lys-83 trinitrophenylation in the apo state (Figure 3A). It slightly decreases the rate of the reaction in the presence of nucleotides (Figure 3B,C). However, the inhibitory effect of MgATP on the modification was stronger than that of MgATPγS also in the presence of PEG. This indicates that in the ATPase cycle S1 is predominantly in the M**·ADP·P_i state in the aggregate. Thus, aggregation does not inhibit the M*ATP → M**·ADP·P_i, i.e., the open → closed transition.

Alkylation of Cys-707 (SH_1) by IAEDANS in the Presence of PEG. The bent α-helix containing Cys-707 (SH_1), which connects the converter region with the rest of the motor domain, is one of the structural elements responsible for transduction of conformational changes during the ATPase cycle of S1 (*4*). The modification of the SH_1 thiol results in the loss of in vitro myosin motility (*36*) and a significant increase in Ca- and Mg-activated and a decrease in K(EDTA)-activated ATPase activity of S1 (*37*). The rate of alkylation of SH_1 thiol with IAEDANS is accelerated by nucleotides. The acceleration is greater when S1 is in the open M*ATP state, mimicked by MgATPγS, than when the closed M**ADP·P_i state is the most populated one in the presence of MgATP (*38*). We studied the effect of 20% PEG-6000-caused aggregation on the alkylation of SH_1 thiol with IAEDANS by assaying the Ca-activated ATPase activity (assayed at high ionic strength, where there is no PEG inhibition) of S1 (Figure 4). The modification increased the Ca-activated ATPase activity, and the increase was somewhat smaller in the presence than in the absence of PEG. The addition of MgATP and MgATPγS further augmented the rate and extent of increase in Ca-ATPase activity; however, the increase was significantly higher with MgATPγS than with MgATP, in both the presence and absence of PEG. This finding is in agreement with the results obtained on the formation and dissociation of trapped S1−phosphate analogue complexes and the modification of Lys-83, i.e., that the closed M**·ADP·P_i state is the most populated at crowding conditions.

S1 Volume and Surface Area in M, M, and M** Conformations.* S1 aggregation induced by PEG should affect

Table 3: QSAR Properties of Homology Modeled Skeletal S1 in Three Conformations

form	id[a]	volume (Å^3)	surface area (Å^2)
M	2mys	260037	39771
M*	1b7t	268631	41375
M**	1br1	259645	38461

[a] Protein Data Bank identification number of the crystal structure used in the homology modeling of the corresponding skeletal S1 structure.

ATPase activity kinetics if conformational change accompanies hydrolysis (*39*). In particular, a conformation that increases volume, surface area, or both will be resisted by the forces stabilizing the aggregate since the aggregated S1 is confined by the interaction with its neighbors. Evidence for a shape change in S1 comes from the crystal structures that show large conformation differences between apo and bound or trapped nucleotide analogue forms (*3*, *4*, *20*). We computed the volume and surface area of skeletal myosin representations of the M, M*, and M** conformations to estimate the effect of the conformation change on these parameters.

The skeletal myosin sequence, including the essential light chain, was homology modeled into the M, M*, and M** conformations using the skeletal (*20*), scallop (*4*), and smooth muscle myosin (*3*) crystal structures, respectively, as described in Materials and Methods. The volume and surface areas of these structures were tabulated using QSAR also as described in Materials and Methods, and the results are summarized in Table 3. Table 3 shows that the volumes and surface areas of the conformations are in the order M* > M > M**. Surface area makes the more dramatic change from M* to M** (~8% compared to ~3% for volume) as expected for a structure that becomes more extended. These findings suggest, in agreement with the other observations described, that transitions from the M** predominant intermediate should be inhibited in the aggregated form because any conformation change accompanying the transition will increase volume and surface area.

DISCUSSION

PEG is a cosolvent added to protein solutions to influence the protein solubility (*22*). For several different proteins tested, PEG was shown to lower the protein solubility and induce aggregation by the steric exclusion mechanism (*22*, *23*, *40*). Steric exclusion preferentially excludes PEG from a volume surrounding the protein due to PEG's size such that higher molecular weight PEG molecules exclude a larger volume around the protein. In this case, the predominant PEG−protein interaction is repulsive, leading to aggregation or the salting out of the protein. Higher molecular weight PEG is the more effective salting out cosolvent. Our data suggest PEG−S1 interact via the steric exclusion mechanism since the reversal of PEG-induced S1 aggregation by KCl requires increasing KCl for larger molecular weight PEG.

Highsmith et al. (*12*) found that the reversible PEG-induced S1 aggregation is accompanied by the loss of its Mg-mediated ATPase activity. KCl (0.5 M), which has no effect on the excluded volume, prevents the PEG-induced aggregation of S1, presumably because high ionic strength prevents the attractive electrostatic interactions between the S1 molecules. This KCl concentration abolishes also the PEG inhibition of the Mg-mediated ATPase activity of S1, indicating that the aggregation and not the presence of the PEG is responsible for the inhibition of the Mg-ATPase activity of S1. Thus there appears to be a causal relationship between aggregation and the loss of enzymatic activity.

Our aim was to identify the step in the ATPase cycle of S1 (Scheme 1) that is inhibited by the aggregation of the protein. We could exclude the first two steps in Scheme 1 (binding of ATP and the subsequent isomerization) from those inhibited by the aggregation since it was shown by Highsmith et al. (*12*) that ATP binds to S1 and increases its tryptophan fluorescence intensity in the absence and presence of PEG-induced aggregation. We found that the aggregation also does not affect the hydrolysis of ATP (step 3 in Scheme 1) because the formation of the S1·MgADP·V_i and S1·MgADP·AlF_4 complexes mimicking the M**·ADP·P_i state proceeds unaffected in the presence of 20% PEG-6000. Moreover, the time course of the chemical modification of Lys-83 and Cys-707 in PEG-aggregated S1, in the presence of ATPγS, when S1 is in the M*ATP state (*35*), is faster than in the presence of ATP. According to our former results (*29*), this indicates that in the presence of ATP the M**·ADP·P_i posthydrolysis state is the most populated intermediate and, therefore, the hydrolysis step in the ATPase cycle is not inhibited by S1 aggregation. Finally, the dissociation of the S1·MgADP·V_i and S1·MgADP·AlF_4 complexes is extremely slow in the presence of PEG (Table 2), indicating clearly that the transition from the M**·ADP·P_i state, i.e., the dissociation of phosphate, is inhibited by the aggregation of S1.

In the Mg-mediated S1 ATPase cycle the dissociation of phosphate from the closed M**·ADP·P_i state is coupled to a 70 deg swing of the lever arm during which myosin conformation transits from the closed to open form (*5*). PEG-induced volume exclusion has been shown to affect those steps of enzyme reactions, coupled with conformation changes that alter protein volume and surface area (*41*). According to our calculations the molecular volume and surface area of S1 are the smallest in the ATPase cycle in the closed M** state and should be favored under the conditions of volume exclusion. Thus the volume exclusion conditions will inhibit the swing of the lever arm necessary to exit the M** conformation. Assuming that lever arm movement and the M**·ADP·P_i to M*·ADP transition are tightly coupled, inhibition of the lever arm movement will likewise inhibit phosphate dissociation. In the absence of tight coupling the observed PEG-induced inhibition of phosphate release would depend on the unlikely possibility that S1 aggregation somehow causes this effect directly.

According to Minton (*39*), if the overall rate of the reaction is limited by the rate with which the transition state complex decays to products, which is the case in S1 ATPase activity, then crowding would be expected to enhance the relative abundance of the transition state complex and hence the forward reaction rate. However, during S1 ATPase activity the decay rate of the predominant state is not enhanced but reduced by the aggregation. This indicates again that not the chemical process (the dissociation of phosphate) but the coupled conformation change is inhibited directly by the PEG-induced volume exclusion.

PEG-induced interactions between S1's in solution model the crowded conditions experienced by the myosin heads in a muscle fiber. We found, in agreement with Highsmith et al. (*12*), that under crowded conditions in solution the MgATPase activity of myosin is inhibited in the absence of actin. It is conceivable that also in muscle the volume exclusion contributes to the observed very low level of myosin ATPase activity under resting conditions, when myosin cross-bridges are dissociated from actin.

Our work shows that in situ interactions could influence steps critical in the contraction cycle. It is widely recognized that cross-bridge strain-dependent rate parameters for binding and release from actin are important to the native assembled system but difficult to emulate in the in vitro assay. We now suggest that one must likewise acknowledge a similar situation for the thermodynamic effects on cross-bridge conformation due to the excluded volume in a muscle fiber. The latter is not emulated in vitro in the absence of PEG and might be the source of discrepancies in force development reported between probe- modified cross-bridges in muscle fibers (*42*) and probe-modified myosin in the in vitro motility assay (*43*).

In summary, we present evidence suggesting that S1 aggregation induced by PEG restrains mechanically the lever arm movement from the closed to the open position, and because of the tight coupling, this prevents the M**ADP·P_i to M*ADP transition and inhibits the Mg-ATPase activity of S1.

ACKNOWLEDGMENT

We are grateful to Dr. Emil Reisler for comments and critical reading of the manuscript.

REFERENCES

1. Fisher, A. J., Smith, C. A., Thoden, J. B., Smith, R., Sutoh, K., Holden, H. M., and Rayment, I. (1995) *Biochemistry 34*, 8960−8972.
2. Dominguez, R., Freyzon, Y., Trybus, K. M., and Cohen, C. (1998) *Cell 94*, 559−571.
3. Houdusse, A., Kalabokis, V. N., Himmel, D., Szent-Gyorgyi, A. G., and Cohen, C. (1999) *Cell 97*, 459−470.
4. Houdusse, A., Szent-Gyorgyi, A. G., and Cohen, C. (2000) *Proc. Natl. Acad. Sci. U.S.A. 97*, 11238−11243.
5. Geeves, M. A., and Holmes, K. C. (1999) *Annu. Rev. Biochem. 68*, 687−728.
6. Bagshaw, C. R., and Trentham, D. R. (1974) *Biochem. J. 141*, 331−349.
7. Highsmith, S., and Eden, D. (1990) *Biochemistry 29*, 4087−4093.
8. Mendelson, R. A., Schneider, D. K., and Stone, D. B. (1996) *J. Mol. Biol. 256*, 1−7.
9. Aguirre, R., Lin, S. H., Gonsoulin, F., Wang, C. K., and Cheung, H. C. (1989) *Biochemistry 28*, 799−807.
10. Cheung, H. C., Gryczynski, I., Malak, H., Wiczk, W., Johnson, M. L., and Lakowicz, J. R. (1991) *Biophys. Chem. 1*, 1−17.
11. Suzuki, Y., Yasunaga, T., Ohkura, R., Wakabayashi, T., and Sutoh, K. (1998) *Nature 396*, 380−383.
12. Highsmith, S., Duignan, K., Franks-Skiba, K., Poloshukhina, K., and Cooke, R. (1998) *Biophys. J. 74*, 1465−1472.
13. Grazi, E., Cintio, O., Magri, E., and Trombetta, G. (1999) *Biophys. J. 76*, 3349−3350.
14. Highsmith, S., Duignan, K., Franks-Skiba, K., Poloshukhina, K., and Cooke, R. (1999) *Biophys. J. 76*, 3351.
15. Tonomura, Y., Appel, P., and Morales, M. F. (1966) *Biochemistry 5*, 515−521.
16. Weeds, A. G., and Taylor, R. S. (1975) *Nature (London) 257*, 54−56.
17. Kodama, T., Fukui, K., and Kometani, K. (1986) *J. Biochem. 99*, 1465−1472.
18. Peyser, Y. M., Ben-Hur, M., Werber, M. M., and Muhlrad, A. (1996) *Biochemistry 35*, 4409−4416.
19. Bodor, N., Gabanyi, Z., and Wong, C.-K. (1986) *J. Am. Chem. Soc. 111*, 3783−3786.
20. Rayment, I., Rypniewski, W. R., Schmidt-Base, K., Smith, R., Tomchick, D. R., Benning, M. M., Winkelmann, D. A., Wesenberg, G., and Holden, H. M. (1993) *Science 261*, 50−58.
21. Martí-Renom, M. A., Stuart, A. C., Fiser, A., Sánchez, R., Melo, F., and Sali, A. (2000) *Annu. Rev. Biomol. Struct. 29*, 291−325.
22. Arakawa, T., and Timasheff, S. N. (1985) *Methods Enzymol. 114*, 49−77.
23. Bhat, R., and Timasheff, S. N. (1992) *Protein Sci. 1*, 1133−1143.
24. Werber, M. M., Peyser, Y. M., and Muhlrad, A. (1992) *Biochemistry 31*, 7190−7197.
25. Phan, B., and Reisler, E. (1992) *Biochemistry 31*, 4787−4793.
26. Kubo, A., Tokura, S., and Tonomura, Y. (1960) *J. Biol. Chem. 235*, 2835−2839.
27. Mornet, D., Pantel, P., Bertrand, R., Audemard, E., and Kassab, R. (1980) *FEBS Lett. 117*, 183−188.
28. Hozumi, T., and Muhlrad, A. (1981) *Biochemistry 20*, 2945−2950.
29. Ajtai, K., Peyser, Y. M., Park, S., Burghardt, T. P., and Muhlrad, A. (1999) *Biochemistry 38*, 6428−6440.
30. Muhlrad, A., and Takashi, R. (1981) *Biochemistry 20*, 6749−6754.
31. Fabian, F., and Muhlrad, A. (1968) *Biochim. Biophys. Acta 162*, 596−603.
32. Muhlrad, A., Peyser, Y. M., Nile, M., Ajtai, K., Reisler, E., and Burghardt, T. P. (2003) *Biophys. J. 84*, 1047−1056.
33. Tonomura, Y., Yoshimura, J., and Onishi, T. (1963) *Biochim. Biophys. Acta 70*, 698−704.
34. Muhlrad, A., and Fabian, F. (1970) *Biochim. Biophys. Acta 216*, 422−427.
35. Goody, R. S., and Hofman, W. (1980) *J. Muscle Res. Cell Motil. 1*, 101−115.
36. Root, D. D., and Reisler, E. (1992) *Biophys. J. 63*, 730−740.
37. Sekine, T., Barnett, L. M., and Kielley, W. W. (1962) *J. Biol. Chem. 244*, 4406−4412.
38. Phan, B. C., Peyser, Y. M., Reisler, E., and Muhlrad, A. (1997) *Eur. J. Biochem. 243*, 636−642.
39. Minton, A. P. (1981) *Biopolymers 20*, 2093−2120.
40. Arakawa, T., and Timasheff, S. N. (1985) *Biochemistry 24*, 6756−6762.
41. Minton, P. A. (2001) *J. Biol. Chem. 276*, 10577−10580.
42. Burghardt, T. P., Garamszegi, S. P., and Ajtai, K. (1997) *Proc. Natl. Acad. Sci. U.S.A. 94*, 9631−9636.
43. Bobkov, A. A., Bobkova, E. A., Homsher, E., and Reisler, E. (1997) *Biochemistry 36*, 7733−7738.

BI0350093